Progress in Agricultural Engineering Sciences 18 (2022) 1, 33–59
DOI: 10.1556/446.2022.00045

AKADÉMIAI KIADÓ

Thermal degradation and kinetic studies of redwood (*Pinus sylvestris* L.)

N. ANTER[1], M. Y. GUIDA[1*], M. KASBAJI[2,3], A. CHENNANI[1], A. MEDAGHRI-ALAOUI[1,4], E. M. RAKIB[1,5] and A. HANNIOUI[1,4]

[1] Laboratory of Organic and Analytical Chemistry (LCOA), Faculty of Sciences and Techniques (FST-BM), University of Sultan Moulay Slimane (USMS), 23000, Béni-Mellal, Morocco

[2] Laboratory of Engineering in Chemistry and Physics of Matter, Faculty of Sciences and Techniques (FST-BM), University of Sultan Moulay Slimane (USMS), 23000, Béni-Mellal, Morocco

[3] Laboratory of Chemical Processes and Applied Materials, Polydisciplinary Faculty (FP-BM), University of Sultan Moulay Slimane (USMS), 23000, Béni-Mellal, Morocco

[4] Department of Chemistry and Environment, Faculty of Sciences and Techniques (FST-BM), University of Sultan Moulay Slimane (USMS), 23000, Béni-Mellal, Morocco

[5] Higher School of Technology (EST-FBS), EST-Fkih Ben Saleh, University of Sultan Moulay Slimane (USMS), 23000, Béni-Mellal, Morocco

ORIGINAL RESEARCH PAPER

Received: March 19, 2022 • **Accepted:** May 30, 2022

ABSTRACT

In this scientific paper, thermochemical conversion of redwood (RW) was studied. Using the thermogravimetric analysis' technique (TGA), the thermal behavior of RW samples was examined at four heating rates ranging from 5 to 20 K min^{-1} in inert atmosphere between 300 and 900 K. Two main objectives have been set for this study; the first one was the determination of the kinetic decomposition parameters of RW (*Pinus sylvestris* L.), and the second one was the study of the variation of characteristic parameters from the TG-DTG curves of the main RW's components, such as; cellulose, hemicellulose and lignin. The kinetic analysis was performed using three isoconversional methods (Vyazovkin (VYA), Friedman (FR) and

---

[*] Corresponding author. E-mail: myassineguida@gmail.com, guida.yassine@gmail.com

Flynn-Wall-Ozawa (FWO)), Avrami theory method and the Integral master-plots ($Z(x)/Z(0.5)$) method to estimate activation energy (E_a), reaction order (n), pre-exponential factor (A) and model kinetic ($f(x)$) for the thermal decomposition of cellulose, hemicellulose and lignin components.

The DTG and TG curves showed that three stages identify the thermal decomposition of RW, the first stage corresponds to the decomposition of hemicellulose and the second stage corresponds to the cellulose, while the third stage corresponds to the lignin's decomposition. For the range of conversion degree (x) investigated ($0.1 \leq x \leq 0.7$), the mean values of apparent activation energies for RW biomass were 127.60–130.65 KJ mol^{-1}, 173.74–176.48 KJ mol^{-1} and 197.21–200.36 KJ mol^{-1} for hemicellulose, cellulose and lignin, respectively. Through varied temperatures from 550 to 600 K for hemicellulose, from 600 to 650 K for cellulose and from 750 to 800 K for lignin, the corresponding mean values of reaction order (n) were 0.200 for hemicellulose, 0.209 for cellulose and 0.047 for lignin. The pre-exponential factor's average values for three components of RW ranges from 0.08×10^{12} s^{-1} to 2.5×10^{12} s^{-1} ($A_{\text{hemicellulose}} = 1.09 \times 10^{12}$ s^{-1}), 0.10×10^{14} s^{-1} to 0.28×10^{14} s^{-1} ($A_{\text{cellulose}} = 0.17 \times 10^{14}$ s^{-1}) and 3.07×10^{16} s^{-1} to 3.69×10^{16} s^{-1} ($A_{\text{lignin}} = 3.33 \times 10^{16}$ s^{-1}), respectively. The experimental data of RW had overlapped the D_4, D_2 and F_3 in the conversion degree of 10–30%, 30–55% and 55–70% for the three components, respectively.

KEYWORDS

thermogravimetric analysis, redwood, kinetic study, isoconversional models, master-plots models

INTRODUCTION

The world today is suffering from several environmental problems that affect the quality of human life (Shang et al., 2013). Due to the overuse of fossil fuels, the environment knows a large deterioration, a radical degradation and transformation from carbon dioxide (CO_2) and methane (CH_4) emissions (Xiao et al., 2017; Pimenta et al., 2018). In this context, lignocellulosic biomass presents a good solution and a right replacement to fossil fuels by advantage of its large quantity, low sulfur and nitrogen contents, environment friendly character and CO_2 neutral energy source (Guida et al., 2021; Malakar et al., 2021). For many years, lignocellulosic biomasses have gained and attracted a lot of interest; they have been investigated in several researches with the purpose to use it as renewable source of energy that can be utilized in different fields and aspects. From literature point of view (Benedeck et al., 2018; Yanting and Liyun, 2011; Bayramzadeh and Aghaei, 2020), there are several types of lignocellulosic biomasses that are composed from cellulose, lignin and hemicellulose contents, such as; organic biomass waste, forest biomass residues, agricultural biomass, energy crops biomass, etc. Among these biomass' types, woody biomass has attracted a lot of researchers with the purpose to produce power, liquid fuels and chemical products from various wood biomasses' categories.

Nowadays, thermochemical conversion technologies, such as; pyrolysis, liquefaction, gasification and combustion, present a good alternative that can be used to valorize lignocellulosic woody biomass into bio-oils, bio-chars and fuels gas products (Khan et al., 2020; Minkova et al., 2001; Uzun et al., 2007). The pyrolysis technology is the main promising thermochemical conversion method for conversion woody biomass. This method 'pyrolysis' is based on chemical degradation of lignocellulosic biomass under effect of heat 'temperature' in the absence of air and oxygen (O_2) (Guida et al., 2020; Liew et al., 2021). Several researches have been carried out on pyrolysis of various types of lignocellulosic biomass (Ozbay et al., 2001; Zabaniotou, 2010; Huang et al., 2016; Klaas et al., 2020), their results have showed that temperature, heating rate, particle size, moisture, residence time and nature of lignocellulosic biomass, are the parameters that affect the course of pyrolysis experiments and influence on the yields of liquid, solid and gas products. To better understand the pyrolysis reaction, it is necessary and imperative to study the thermal degradation of biomasses' types and evaluate their potential thermochemical valorization process. Thermogravimetric analysis is the main reliable technique used to study the thermal degradation and to estimate and study the kinetic parameters of the thermal process decomposition. Several scientific papers have been published on thermogravimetric analysis of various biomasses' kind (Meshitsuka and Isogai, 1996; Worasuwannarak et al., 2007; Guida et al., 2021; Duan et al., 2020; Ioannidou et al., 2009), they showed that the thermal decomposition of biomass is different from one type to another. As mentioned in Fig. 1a, that presents documents published on thermogravimetric analysis of wood waste during 1978–2021 period, it can be seen that from 1978 to 2000, the number of documents published was low; it does not

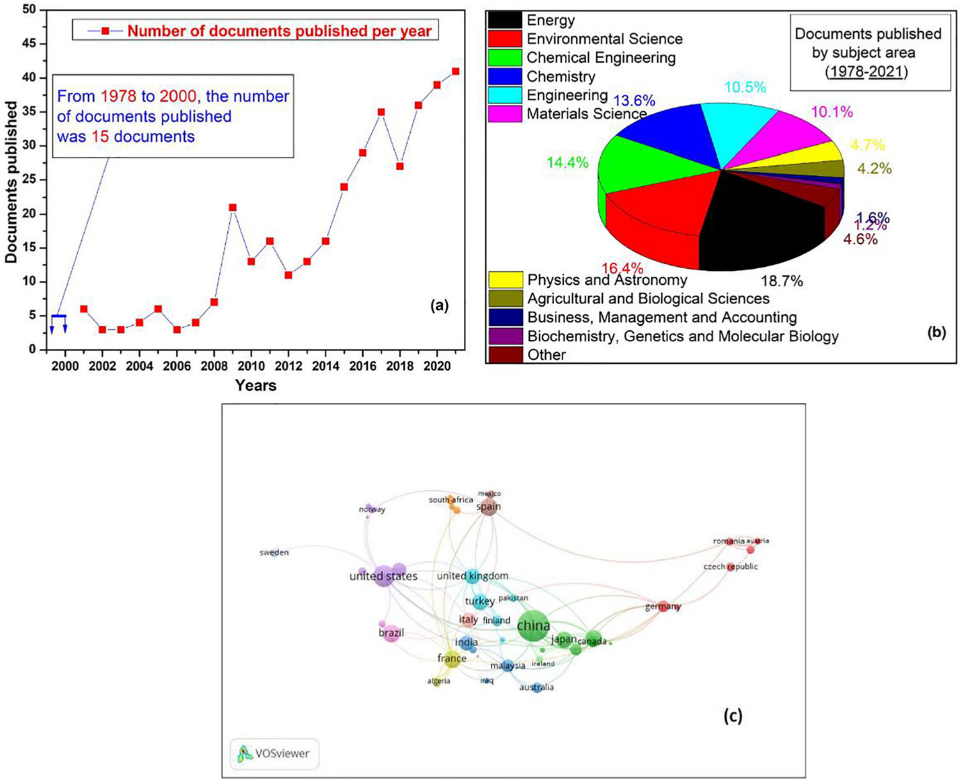

Fig. 1. Documents published on thermogravimetric analysis (TGA) of wood waste during 1978–2021 periods. (a) per year, (b) by subject and (c) network of cooperation based on co-authorship between countries. (Keywords: 'thermogravimetric' AND 'analysis' AND 'of' AND 'wood' AND 'waste') (source: Scopus)

exceed 15 documents. However, from 2000 to 2021, the number of published documents has increased, there was a shift increase of TGA of wood documents studies. Figure 1b shows that energy (18.7%), environmental science (16.4%), chemical engineering (14.4%), chemistry (13.6%), engineering (10.5%) and materials science (10.1%) are the domains and areas which use thermogravimetric analysis of wood biomass between 1978 and 2021. As can be seen in Fig. 1c, the greatest countries that made their researches on thermogravimetric analysis of wood waste are: the United States, China, Germany, Canada, France, the United Kingdom, Spain and Brazil. Morocco is one of the countries that are attracted by TGA of wood biomass. Moroccan cluster contains; France, Burkina Faso, Benin, Algeria, Gabon and Morocco, as mentioned in Fig. 1c.

Previous studies have been made on thermochemical valorization of wood biomass (Chen et al., 2016; Moya et al., 2018; Mafu et al., 2018; Zhou et al., 2013). Zhou et al. (2013) have studied the pyrolysis simulation of poplar wood biomass between 323 and 1273 K with heating rate of 10 K/min; they have showed that pyrolysis process of poplar wood biomass could be divided into three phases. Chen et al. (2016) have shown that weight loss of woody biomass increased with increasing the pyrolysis temperature. According to Moya et al. (2018) and Mafu et al. (2018), temperature of pyrolysis plays an important role in and influences thermal decomposition of woody biomass. Other studies have been carried out on the kinetic parameters of wood biomass degradation (Slopiecka et al., 2012; Poletto et al., 2016; Grønli et al., 2002; Mishra et al., 2015). Using thermogravimetric technique, the pyrolysis of poplar wood biomass was studied by Slopiecka et al. (2012); they have found that TGA of wood biomass can be divided into three zones that are drying, active pyrolysis and passive pyrolysis. The authors have used three methods; Kissinger, FWO and KAS models, activation energies values obtained were 157.27 KJ mol^{-1}, 153.92 KJ mol^{-1} and 158.58 KJ mol^{-1}, from KAS, Kissinger and FWO methods, respectively. According to Grønli et al. (2002), hardwoods and softwoods biomasses have been studied. The authors have showed that degradation of all biomass wood types occurred as three parallel reactions. They divided biomasses studied to hemicellulose, cellulose and lignin compounds. Activation energies obtained from their researches were 100 KJ mol^{-1} for hemicelluloses, 236 KJ mol^{-1} for cellulose and 46 KJ mol^{-1} for lignin. Poletto et al. (2016) have studied pine wood biomass using TGA. They found that thermal decomposition of wood biomass is due to D_3 mechanism, which means a three dimension diffusion process. Misha et al. (2015) have studied pine wood biomass degradation. The results obtained from their work have showed that the thermal decomposition mechanism was governed by D_2 diffusion. The values of activation energy obtained were 134.32 KJ mol^{-1}, 146.89 KJ mol^{-1}, and 155.76 KJ mol^{-1} for hemicellulose component, cellulose component and lignin component, respectively. Anca-Couce et al. (2016) have shown that activation energies of lignocellulosic biomass are different; it depends on nature of biomasses. The authors have mentioned that activation energies for cellulose ranged from 114 KJ mol^{-1} to 288 KJ mol^{-1}, for hemicellulose ranged from 34 KJ mol^{-1} to 179 KJ mol^{-1}, while for lignin compound activation energies values ranged from 7 KJ mol^{-1} to 226 KJ mol^{-1}. Other published scientific papers (Antal et al., 1998; Gronli et al., 1999; Anca-Couce et al., 2014; White et al., 2011; Branca et al., 2005; Sànchez-Jiménez et al., 2014) have shown that the nature of biomass studies influences the study of kinetic parameters and the thermal decomposition of the raw material. In our previous studies (Guida et al., 2015, 2017, 2019, 2020, 2021), several types of biomasses have been studied using TGA technique and pyrolysis apparatus. From these scientific works, it has been concluded that the nature of biomass and the amounts of cellulose, hemicellulose and lignin contents have significant influence on the thermal degradation of the biomass' type and on the thermal comportment of all pseudo-components compounds.

Using isoconversional models can show the dependence of activation energies on the reaction's conversion degree, knowing that pyrolysis reaction includes several different reactions that occur at the same reaction time. There are two pyrolysis approaches which describe the thermal decomposition of the wood biomass; the first one considers the biomass as one component and the second one considers the biomass as pseudo-components of different compounds (hemicellulose, cellulose, and lignin). Little scientific works have been reported for thermal composition, kinetic study and mechanism characteristics of biomasses adopting the pseudo-components approach. Especially, redwood (*Pinus sylvestris* L.) kinetic and mechanistic analyses using the second approach (pseudo-components) have not been reported yet.

The main objectives of this scientific study are to determine qualitatively and quantitatively the thermal degradation characteristics of *P. sylvestris* L. species of RW. First of all, thermogravimetric analysis of RW was recorded using a device named 'thermogravimetric analyzer' at four heating rates of 5, 10, 15 and 20 K min^{-1}. Furthermore, based on raw thermogravimetric results, isoconversional methods and Avrami theory were used to determine energy of activation values and reaction order. Finally, using the integral master plots, the reactions models for hemicellulose, cellulose and lignin components were determined during the TGA of *P. sylvestris* redwood.

MATERIALS AND METHODS

Materials

In this study, the redwood samples were obtained from Beni-Mellal area (central zone) that is located about 304 Km of Rabat and 200 Km of Marrakech (Morocco). The samples of RW biomass used in this work were *P. sylvestris* L. species. These samples were obtained from the Beni-Mellal's carpentry of construction that is located in the middle of the city. The samples collected were crushed and sieved with a particle size of 0.10–0.20 mm. Volatile matter content, Ash and Moisture contents were determined using TGA analysis. The fixed carbon content was calculated using the following formula:

$$\text{Fixed carbon}(\text{wt\%}) = 100 - (\text{Volatile matter}(\text{wt\%}) + \text{Ash}(\text{wt\%}))$$

The ultimate, proximate and fiber analyses of *P. sylvestris* species samples are depicted in Table 1.

Thermogravimetric analysis experiments

RW samples used in this study were exposed to thermogravimetric analysis in an inert atmosphere of nitrogen (N_2). Rheometrix scientific STA 1500 analyzer was utilized to trace the mass loss change versus temperature (TG) and to evaluate kinetic parameters of redwood biomass's decomposition, through the pyrolysis reaction course. DTG (derivative thermogravimetry) and TG curves were obtained at heating rates of 5 K min^{-1}, 10 K min^{-1}, 15 K min^{-1} and 20 K min^{-1}, between 300 and 900 K. Nitrogen flow rate was 60 mL min^{-1}. All samples' quantities used in this study averaged 20 mg. The experiments of TGA were carried out two times for better reproducibility and accuracy of results.

Table 1. Proximate, ultimate and fiber analyses of redwood

Characteristics		Percentage
Proximate analysis (wt%)	Moisture content	4.8
	Volatile matter	76.83
	Ash	4.19
	Fixed carbon	18.98
Ultimate analysis (wt%)	Carbon	44.59
	Hydrogen	5.1
	Nitrogen	0.51
	Sulfur	0.44
	Oxygen	45.17
Fiber analysis (wt%)	Hemicellulose	29.07
	Cellulose	42.51
	Lignin	19.66
	Extractive	8.76
H/C molar ratio		1.372
O/C molar ratio		0.759
Empirical formula		$CH_{1.372}O_{0.759}N_{0.009}$
Higher heating value (MJ kg^{-1})		17.82

Kinetic methods and theory

Woody biomass' thermal decomposition is a heterogeneous reaction, it can be modeled as:

$$\text{Woody biomass(s)} - - - - - > \text{Volatile}_{(\text{gases+tar})} + \text{char}_{(\text{solid residue})}$$

There are two types of kinetic analysis models; the modelfiting models and the isoconversional models. Several studies (Guida et al., 2015; Mu et al., 2015; Vyazovkin, 2006; Watt et al., 2020; Phuakpunk et al., 2020; Mullen et al., 2010) have demonstrated that isoconversional models are preferred and used in thermochemical study's researches. There are two reasons for this preference. Firstly, these models are sufficiently flexible to allow for a change in mechanism during a reaction. Secondly, the limitations of mass transfer are reduced by the use of multiple heating rates (generally, three or four heating rates).

Biomass conversion can be calculated as:

$$x = \frac{m_0 - m_t}{m_0 - m_f} \tag{1}$$

Where, mt is the sample mass at a given time t, m_0 and m_f refer to mass values at the beginning and the end of the mass loss rate. The heterogeneous rate solid state reactions can be generally described as follows:

$$\frac{dx}{dt} = K(T) \times f(x) \tag{2}$$

According to Arrhenius equation, the rate constant is described by equation (3), as follows:

$$K(T) = A \times \exp\left(\frac{-E}{R \times T}\right) \tag{3}$$

f(x) is the reaction model that describes the reaction's mechanism. T is the temperature, E is the activation energy, A is the Arrhenius parameter, and R is the gas constant. Using equations (2) and (3), the reaction rate can be written as follows:

$$\frac{dx}{dt} = A \times \exp\left(\frac{-E}{R \times T}\right) \times f(x) \tag{4}$$

Friedman method (FR)

This method is considered the most used general differential isoconversional method. It is directly based on equation (4) (Friedman, 1964). Using the direct integration of equation (4), it gives the following equation:

$$ln\left(\frac{dx}{dt}\right) = ln(f(x) \times A) - \frac{E}{R \times T} \tag{5}$$

From this equation (5), it is possible to obtain the apparent activation energy over a wide range of conversion degree *(x)* by plotting $ln(dx/dt)$ against $1/T$ under a given value of conversion degree.

Flynn-Wall-Ozawa (FWO)

In this method, Doyle's approximation was used (Doyle, 1961). It can be transformed into non isothermal rate expression that describes reaction rate at a constant heating rate *(β)*, as mentioned in equations (6) and (7):

$$\beta = \frac{dT}{dt} \tag{6}$$

$$\frac{dx}{dt} = \frac{A}{\beta} \times \exp\left(\frac{-E}{R \times T}\right) \times f(x) \tag{7}$$

Using equation (7) and integrating it, it can give equation (8) above:

$$\int_0^x \frac{dx}{f(x)} = g(x) = \frac{A}{\beta} \times \int_{T_0}^{T} \exp\left(\frac{-E}{R \times T}\right) dT \tag{8}$$

In this equation (8), *g(x)* is the integral kinetic function or integral reaction model when its form is mathematically defined, as can be seen in Table 2.

Using this method, activation energy can be obtained by plotting *ln(β)* versus $1/T$, as can be seen in equation (9):

$$ln(\beta) = ln\left(\frac{A \times E}{R \times g(x)}\right) - 5.331 - 1.052 \times \frac{E}{R \times T} \tag{9}$$

Table 2. Reaction models applied to simulate the reaction kinetics in heterogeneous solid-state system

Model		Integral form *g(x)*	Differential form *f(x)*
Reaction-order models			
First-order	*F1*	$-ln(1-x)$	$(1-x)$
Second-order	*F2*	$(1-x)^{-1}-1$	$(1-x)^2$
Third-order	*F3*	$[(1-x)^{-2}-1]/2$	$(1-x)^3$
Diffusion models			
1-D diffusion	*D1*	x^2	$1/2x$
2-D diffusion	*D2*	$[(1-x)ln(1-x)]+x$	$[-ln(1-x)]^{-1}$
3-D diffusion, Jander	*D3*	$[1-(1-x)^{1/3}]^2$	$3(1-x)^{2/3}/[2(1-(1-x)^{1/3})]$
Ginstling-Brounshtein	*D4*	$1-(2x/3)-(1-x)^{2/3}$	$3/[2((1-x)^{-1/3}-1)]$
Geometrical contraction models			
Contracting area	*R2*	$[1-(1-x)^{1/2}]$	$2(1-x)^{1/2}$
Contraction volume	*R3*	$[1-(1-x)^{1/3}]$	$3(1-x)^{2/3}$
Nucleation models			
Power law	*P2*	$x^{1/2}$	$2x^{1/2}$
Power law	*P3*	$x^{1/3}$	$3x^{2/3}$
Power law	*P4*	$x^{1/4}$	$4x^{3/4}$
Avrami-Erofeyev	*A2*	$[-ln(1-x)]^{1/2}$	$2(1-x)[-ln(1-x)]^{1/2}$
Avrami-Erofeyev	*A3*	$[-ln(1-x)]^{1/3}$	$3(1-x)[-ln(1-x)]^{2/3}$
Avrami-Erofeyev	*A4*	$[-ln(1-x)]^{1/4}$	$4(1-x)[-ln(1-x)]^{3/4}$

Vyazovkin method (VYA)

This method was developed by Vyazovkin and Lesnikovick (Vyazovkin et al., 1988). It can distribute both complex and simple reactions to be estimated and evaluated.

In equation (8), since $E/2RT >> 1$, the temperature integral could be approximated by equation (10):

$$\int_{T_0}^{T} \exp\left(\frac{-E}{R\times T}\right)dT \approx \frac{R}{E}\times T^2\times \exp\left(\frac{-E}{R\times T}\right) \qquad (10)$$

By taking the logarithm and substituting the temperature integral, equation (11) can be obtained:

$$ln\left(\frac{\beta}{T_x^2}\right) = ln\left(\frac{R\times A}{E\times g(x)}\right) - \frac{E}{R\times T} \qquad (11)$$

By plotting $ln(\beta/T^2{}_x)$ versus $1/T$, activation energy *(E)* can be obtained as a function of conversion degree *(x)*.

Avrami theory

In order to evaluate the order of reaction, Avrami theory was used in this scientific work (Ozawa, 1965; Liu et al., 2009). Reaction order is a significant parameter to investigate the biomass' pyrolysis characteristic, in addition activation energy. It could be described as:

$$x = 1 - \exp\left(\frac{-K(T)}{\beta^{n}}\right) \tag{12}$$

x, *β* and *K(T)* are the conversion degree, heating rate and Arrhenius equation. Transporting and taking the double logarithm, equation (12) will be transformed into the following equation:

$$ln(-ln(1-x)) = ln(A) - \frac{E}{R \times T} - n \times ln(\beta) \tag{13}$$

By a given temperature *T*, $ln(-ln(1-x))$ versus *ln(β)* at different temperature heating rate can be fitted to a straight line. The slope obtained of the straight line corresponds to *(−n)*.

Pre-exponential factor (A)

By using the Kissinger method (Kissinger, 1957), as can be seen in equation (14). At different heating rates, this method can give activation energy at a wide range of conversion's degree *(x)*. However, by determining the energy of activation at a range of degree of conversion, equation (15) can be used to calculate pre-exponential factor.

$$ln\left(\frac{\beta}{T_m^2}\right) = ln\left(\frac{A \times R}{E}\right) - \frac{E}{R \times T_m} \tag{14}$$

$$A = \frac{\beta \times E \times \exp\left(\frac{E}{R \times T}\right)}{R \times T_m} \tag{15}$$

Thermal degradation mechanism using master plots models

This method uses equation (8) (Doyle, 1965):

$$g(x) = \frac{A}{\beta} \times \int_{T_0}^{T} \exp\left(\frac{-E}{R \times T}\right) dT = \frac{A \times E}{\beta \times R} \times p(u) \tag{16}$$

p(u) is given as:

$$p(u) = \int_{\infty}^{u} -\left(\frac{e^{-u}}{u^2}\right) du \tag{17}$$

$$\mathrm{u} = \mathrm{E}/\mathrm{RT}$$

To obtain the solution of equation *p(u)*, Doyle's approximation was used (Doyle, 1965). From equation (16) and given that; $x = 0.5$ as an orientation it follows:

$$Z(0.5) = \frac{A \times E}{\beta \times R} \times p(u_{0.5}) \tag{18}$$

From equations (16) and (18), the following can be obtained:

$$\frac{Z(x)}{Z(0.5)} = \frac{p(u)}{p(u_{0.5})} = \frac{T^2}{T_{0.5}^2} \times \frac{\exp\left(\frac{-E}{R \times T}\right)}{\exp\left(\frac{-E}{R \times T_{0.5}}\right)} = \frac{g(x) \times f(x)}{g(0.5) \times f(0.5)} \tag{19}$$

Table 2, was used to determine the mechanism type in the thermal decomposition of RW biomass studied. The right side of equation (19) is used to fit and to characterize the experimental curves. By comparing experimental curve with the theoretical curves for each model, the mechanism type can be identified.

RESULTS AND DISCUSSION

P. sylvestris RW biomass' characterization

The ultimate, proximate and fiber analyses were determined which the aim to characterize the raw material used in this scientific study. Table 1 shows the main characteristics of RW biomass used in this study. All the presented results have been shown as mass percentage (wt%). From proximate analysis, the RW biomass has a volatile matter of 76.83 wt%; this value is higher than 70 wt% which indicates that *P. sylvestris* species of RW biomass could produce condensable vapors through pyrolysis experiments. Several studies have shown that volatile matter content is desirable for the pyrolysis process and the ash content varies depending on biomass types. It was determined at 4.5 wt% for switchgrass, 6 wt% for barely straw and 4 wt% for wheat straw (Akhtar et al., 2012; Huang et al., 2016; Mohan et al., 2006) In this study, the ash percentage was 4.19 wt%, comparing this value with other published works values, it can be said that RW biomass has a low percentage. Other works have shown that a higher ash value can affect the mechanism of biomass degradation, because inorganic material which is in ash compound has the ability to affect the pyrolysis mechanism. As far as moisture and fixed carbon contents are concerned, they were 4.8 wt% and 18.98 wt%, respectively. These values obtained in this work are in consistence with other works (Sensoz et al., 2006; Asadullah et al., 2007) that showed that moisture content in lignocellulosic biomass must be below 10 wt%.

From Table 1, it can be seen that cellulose, hemicellulose and lignin's contents were 42.51 wt%, 29.07 wt% and 19.66 wt%, respectively. It can be seen that RW biomass presents a good opportunity for source of renewable energy using pyrolysis conversion technique. Several studies have been published (Guida et al., 2020; Xin et al., 2020; Situmorang et al., 2021) which showed that hemicellulose, cellulose and lignin contents vary depending on the type of lignocellulosic biomasses studied.

From the ultimate analysis, the carbon, oxygen, hydrogen, nitrogen and sulfur contents were 44.59 wt%, 45.17 wt%, 5.1 wt%, 0.51 wt% and 0.44 wt%, respectively. This type of RW biomass with low sulfur and nitrogen contents could be a good nominee for thermochemical conversion technology. They are some researches (Guida et al., 2020; Xin et al., 2020; Situmorang et al., 2021) which have shown that low nitrogen and sulfur amounts in lignocellulosic biomasses imply little amounts of SO_x and NO_x compounds' production during the thermogravimetric and pyrolysis analyses.

Thermal degradation of RW biomass

The thermogravimetric (TG) and derivative thermogravimetry (DTG) curves of RW biomass samples at heating rates of 5 K min^{-1}, 10 K min^{-1}, 15 K min^{-1} and 20 K min^{-1} are presented in

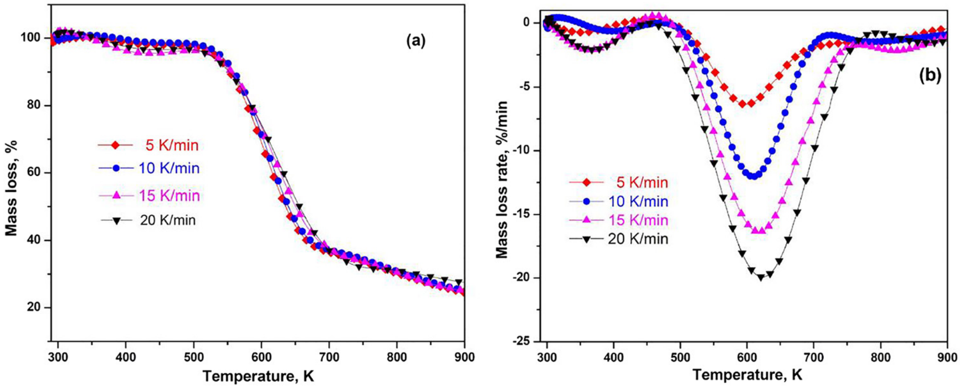

Fig. 2. TG and DTG curves of redwood at different heating rates

Figs 2a and 2b. The thermogravimetric analysis profiles under inert atmosphere (N_2) of *P. sylvestris* biomass obtained are similar to TGA profiles of several types of wood biomass (Anca-Couce et al., 2020; Guida et al., 2017, 2020). The differences exist between this study and other studies that are the nature of the biomasses utilized during the thermal characterization and the composition of wood biomass analyzed. As mentioned above, lignocellulosic biomasses are composed from cellulose, hemicellulose and lignin components. Figures 3a and 3b show that *P. sylvestris* L. biomass is composed from three pseudo-components that are cellulose, hemicellulose and lignin, and each pseudo-component has dissimilar temperatures of degradation. As can be seen in Fig. 3a, the thermochemical degradation of RW biomass has been identified by three thermal zones. As mentioned in Table 3, the first zone occurs in the thermal interval from ambient temperature that is 301 K to around 430–465 K; this zone was linked to the moisture loss and drying of the raw material 'RW biomass' with some light volatile components. The mass loss rate in this first zone was approximately 4.72 wt%, which confirms the result obtained from proximate analysis in characterization section, which showed moisture content of 4.8 wt%. The main decomposition process, which relates to the degradation and devolatilization of cellulose, hemicellulose and lignin, occurred in the second zone that is called 'active zone' in other studies (Guida et al., 2021; Kumar Varma et al., 2019). This second zone has been ranged from 429 to 464 K to around 751–793 K (Table 3a), the mass loss of the main thermogravimetric analysis was 73.11 wt%. After the main decomposition pyrolytic of cellulose, hemicellulose and some lignin, a continuous and slow decomposition mainly ups to 900 K. This continuous and slow degradation occurs in the third zone, which ranged from 751 to 793 K to around 891–897 K. This third zone has been attributed to the degradation of the lignin component (Figs 3b and 3c) and some of carbonaceous compounds 'bio-char' that are in the residues. The residual mass obtained after 897 K was 21.47 wt% for this type of RW biomass. According to these results obtained from this scientific study, it can be seen that temperature plays an important role in the thermal decomposition of the RW biomass. Added to this and as mentioned in Fig. 2b, heating rate is one the most important parameters that must be taken in consideration through thermal degradation study of the biomass. Heating rates affect significantly the maximum degradation rate, when the heating rate increases the maximum of decomposition rate increases, which influences the initial and final decomposition temperatures (Table 3).

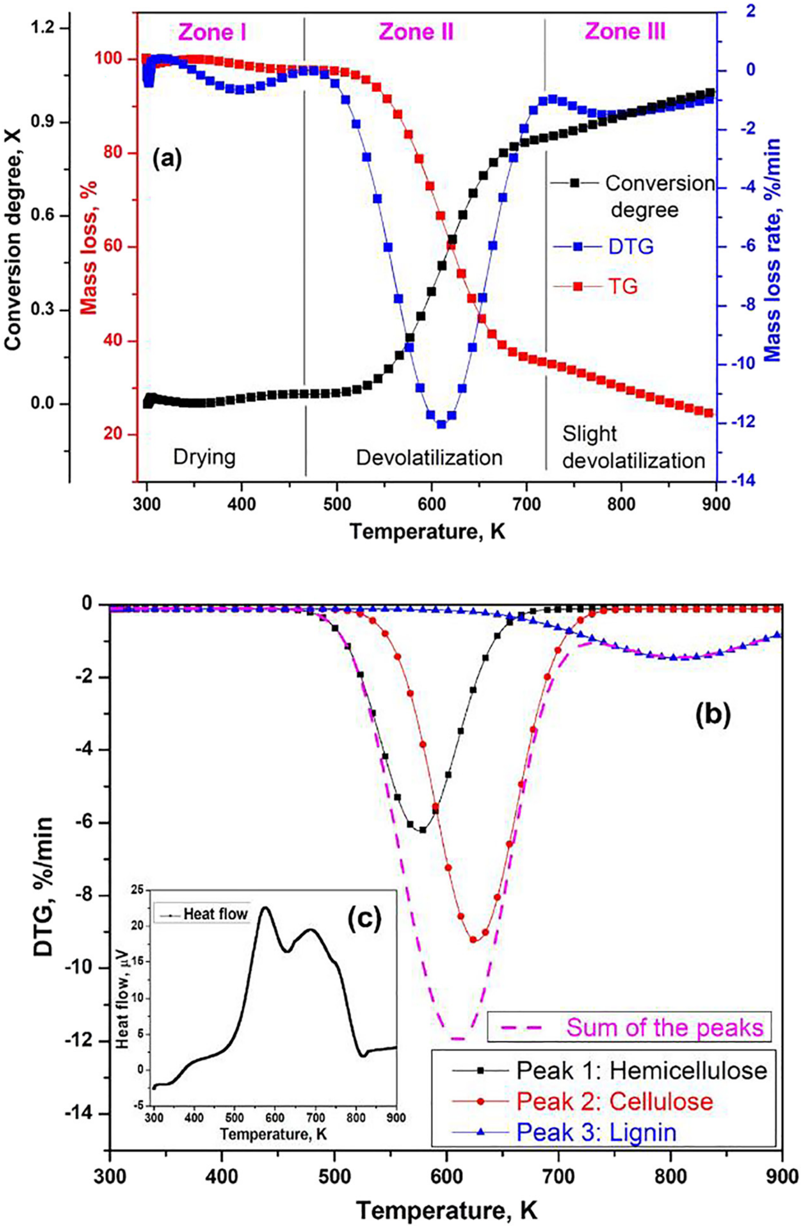

Fig. 3. (a) TG, DTG and conversion degree at 10 K min^{-1}, (b) pyrolysis peaks of RW's components and (c) heat flow of RW at 10 K min^{-1}

As determined in Table 4, the second zone (zone II) can be divided into three stages, stage I, stage II and stage III, which correspond to the initial and final temperatures of hemicellulose,

Table 3. Initial, maximal and final temperatures of the three zones of redwood's decomposition

	Zone I			Zone II			Zone III		
	T_i(K)	T_m(K)	T_f(K)	T_i(K)	T_m(K)	T_f(K)	T_i(K)	T_m(K)	T_f(K)
5 K min^{-1}	300	351	429	429	597	751	751	778	891
10 K min^{-1}	301	394	459	459	612	724	724	788	893
15 K min^{-1}	301	364	461	461	622	774	774	818	894
20 K min^{-1}	300	367	464	464	627	793	793	866	897

Table 4. Characteristic temperatures of hemicellulose, cellulose and lignin components of redwood

	Stage I: hemicellulose			Stage II: cellulose			Stage III: lignin		
	T_i(K)	T_m(K)	T_f(K)	T_i(K)	T_m(K)	T_f(K)	T_i(K)	T_m(K)	T_f(K)
5 K min^{-1}	456	571	693	489	620	761	515	766	801
10 K min^{-1}	473	573	695	510	625	767	581	794	830
15 K min^{-1}	475	574	699	511	634	802	701	810	848
20 K min^{-1}	479	581	701	515	641	807	705	839	879

cellulose and lignin decompositions. As ranging heating rates from 5 K min^{-1} to 20 K min^{-1}, the first stage occurred from 456 to 701 K, the second stage occurred from 489 to 807 K, while the third stage has been ranged from 515 to 879 K. The second zone was the most important zone of degradation. It was characterized by the production of large quantities of volatile compounds. According to these results, several researches have been published on several types of biomasses (Chen et al., 2015; Kumar Varma et al., 2019; Liew et al., 2021; Rout et al., 2016); these works have shown that the profile decomposition of biomass is different and depends on the nature of the raw material used. Kumar Varma et al. (2019), have mentioned that the most important active pyrolysis ranges from 433 to 793 K. Chen et al. (2015), have shown in their work that degradation temperatures of hemicellulose, cellulose and lignin ranged from 414 to 577 K, from 549 to 680 K, and from 653 to 861 K, respectively. Kaur et al. (2018) have shown that the second zone, called 'active zone', refers to the decomposition of cellulose, hemicellulose and lignin components. They mentioned that active zone occurs at temperatures ranging from 433 to 793 K (Kaur et al., 2018).

Activation energy determination

TGA curves were divided into three temperature stages (Figs 3a and 3b). Thermal kinetic analyses of experimental results were limited to the stages of thermal decomposition of hemicellulose, cellulose and lignin. The conversion degrees depending on the pyrolysis' temperature and at heating rates of 5 K min^{-1}, 10 K min^{-1}, 15 K min^{-1} and 20 K min^{-1} have been shown in Figs 4a–c. It can be seen that conversion degrees for cellulose, hemicellulose and lignin pseudo-components increase with the temperature increase. The pyrolysis degradation kinetics during the pyrolysis process of RW biomass has been studied by using Friedman (eq. (5)), Flynn-Wall-Ozawa (eq. (9)) and Vyazovkin (eq. (11)) isoconversional methods. At a wide range of degree of conversions ranging from 10% to 70% ($0.1 \le x \le 0.7$),

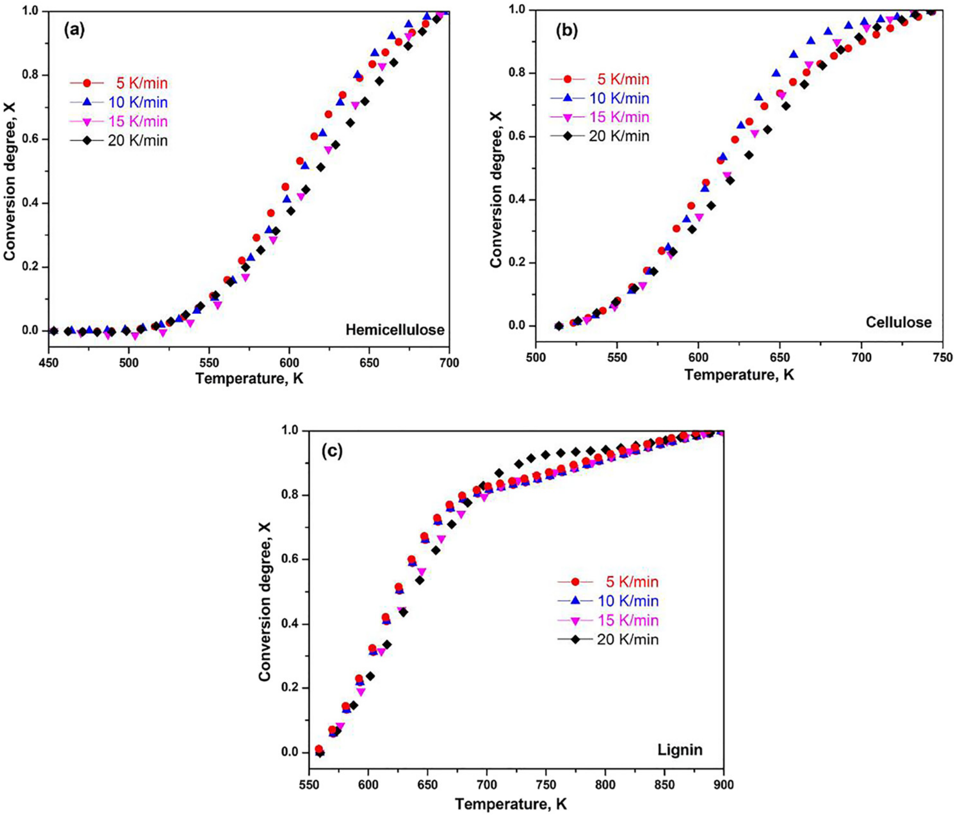

Fig. 4. Variation of conversion degree (x) as a function of temperature at different heating rates for (a) hemicellulose, (b) cellulose and (c) lignin of redwood

with an increment of 5% ($x = 0.05$) for the three stages, the activation energy's values have been calculated and determined.

Using the linear regression method, as indicated in Figs 5–7. The activation energy values were calculated and determined from the fitted straight line's slope *(–E/R)*. For all values sets the linear isoconversional plots of VYA, FR and FWO methods have resulted in a correlation coefficient (R^2) higher than 0.95. The dependence of activation energy values (E_a) on the conversion degree for thermal degradation process of cellulose, hemicellulose and lignin obtained using isoconversional methods is shown in Figs 5–7d. The apparent activation energies have values of 127.6–130.65 KJ mol^{-1} for hemicellulose, 173.74–176.48 KJ mol^{-1}, and 197.21–200.36 KJ mol^{-1} for lignin decomposition of RW biomass. As shown in Table 5, the mean values obtained from FR, FWO and VYA methods were ranging from 130.65 KJ mol^{-1} to 200.36 KJ mol^{-1} for FR method, from 129.56 KJ mol^{-1} to 197.21 KJ mol^{-1} for FWO method and from 127.60 KJ mol^{-1} to 199.54 KJ mol^{-1} for Vyazovkin method. It can be seen that activation energies obtained from FWO and VYA methods give similar values, whereas, activation energy values obtained from FR method were larger than those obtained by VYA and FWO. This

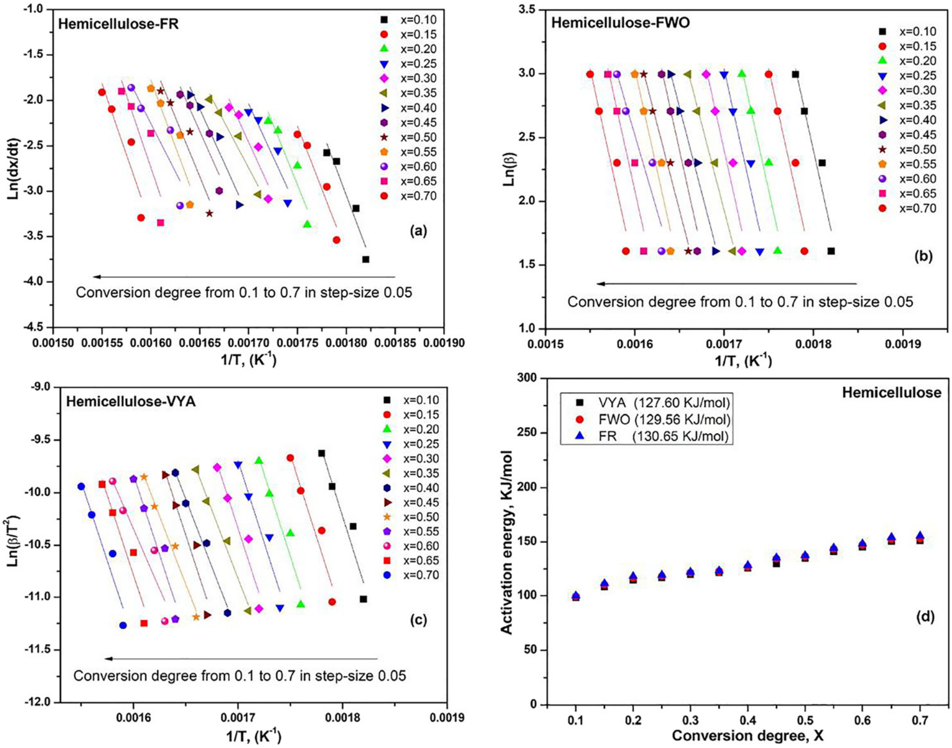

Fig. 5. Regression linear for determining E_a of hemicellulose component by (a) FR, (b) FWO and (c) VYA, (d) the dependence of E_a with the conversion degree (x)

difference in energy of activation can be explained by the error of improper integration in VYA and FWO equations, while FR method uses a very sensitive and instantaneous *(dx/dt)* rate values. It should be noticed that FR method does not use any approximations, despite that, FWO and VYA methods use some approximations and assumptions. Results obtained from this study fit with several studies (Anca-Couce et al., 2014; Chen et al., 2015; Hu et al., 2016; Guida et al., 2020). Anca-Couce et al. (2014) have worked on the determination consistent beech wood biomass pyrolysis kinetics in parallel reaction scheme; they have shown that activation energies obtained were 150.8–179.3 KJ mol^{-1} for hemicellulose, 177.4–190.2 KJ mol^{-1} for cellulose and 203–211.4 KJ mol^{-1} for lignin. According to this, Hu et al. (2016) studied the thermogravimetric kinetic analysis of lignocellulosic biomass; they have shown that the mean activation energies values for the three pseudo-components were 154.55–168.63 KJ mol^{-1} for hemicellulose, 188.14–206.71 KJ mol^{-1} for cellulose and 199.08–221.21 KJ mol^{-1} for lignin, respectively. Chen et al. (2015) have derived activation energies of 175.71–201.6 KJ mol^{-1}, 171.04–179.54 KJ mol^{-1} and 148.12–164.56 KJ mol^{-1} for lignin, cellulose and hemicellulose, respectively. Guida et al. (2020) have worked on thermogravimetric analysis and pyrolysis studies of sawdust wood waste, their results have shown that the mean values of activation energies were 168.34 KJ mol^{-1} from FR method, 153.35 KJ mol^{-1} from VYA method and 168.84 KJ mol^{-1} from FWO method. From

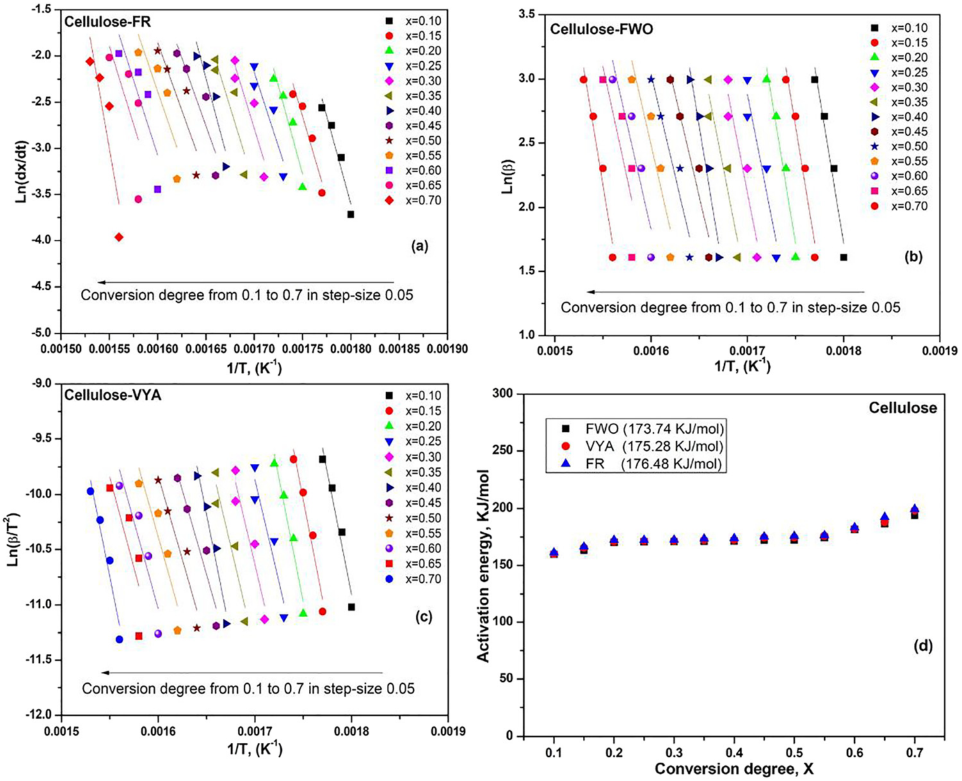

Fig. 6. Regression linear for determining E_a of cellulose component by (a) FR, (b) FWO and (c) VYA, (d) the dependence of E_a with the conversion degree (x)

Table 5, and Figs 5–7, it can be seen that the energies of activations take the order E_a(hemicellulose) < E_a(cellulose) < E_a(lignin), which can indicate that the activation energies for the degradation of hemicellulose are the lowest than that of cellulose and lignin, this result is in coincidence with the work of Cai et al. (2013). Cai et al. (2013) have studied the distribution of model of activation energies for thermal degradation of lignocellulosic biomasses; they have shown an average value of 237–266.6 KJ mol^{-1}, 204.2–212.5 KJ mol^{-1} and 169.7–186.8 KJ mol^{-1} for lignin, cellulose and hemicellulose, respectively.

Determination of reaction order (*n*) and pre-exponential factor (A)

In this study, Avrami theory was used to determine reaction order (n) of hemicellulose, cellulose and lignin decomposition. According to eqation (13), linear regression was used to deduce the order of reaction for the three pseudo-components in three temperatures regions. All the three regions of temperatures were ranging from 550 to 600 K, from 600 to 650 K and from 750 to 800 K for hemicellulose, cellulose and lignin, respectively. As can be seen in Figs 8a–c, for a wide range of pyrolysis temperature T, the plot of $ln(-ln(1-x))$ versus $\ln(\beta)$ at different heating rates of 5 K min^{-1}, 10 K min^{-1}, 15 K min^{-1} and 20 K min^{-1}, could be fitted to a straight line,

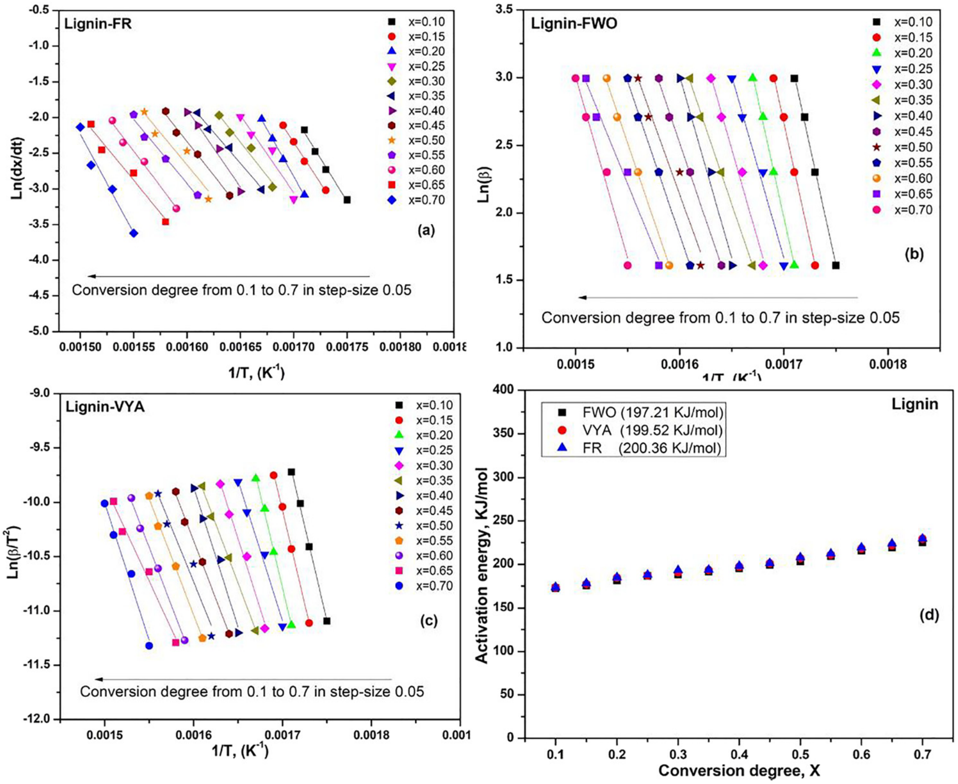

Fig. 7. Regression linear for determining E_a of lignin component by (a) FR, (b) FWO and (c) VYA, (d) the dependence of E_a with the conversion degree (x)

and the line slope corresponds to *(−n)*. The corresponding values of correlation coefficient (R^2) and reaction order deduced from Avrami theory for hemicellulose, cellulose and lignin for *P. sylvestris* RW biomass are listed in Table 6. As presented in Table 6, as the temperatures increase, the reaction order varies depending on the pseudo-components nature. Firstly, hemicellulose's reaction order values have been increased from 0.14 to 0.26 with the temperature increase from 550 to 600 K. It has been shown that hemicellulose reaction order increases with the increasing of pyrolysis temperature. Secondly, a cellulose component has been characterized

Table 5. Average value of E_a obtained for each component of redwood

	Activation energy (E_a), KJ mol^{-1}		
Isoconversional methods	Friedman	FWO	Vyazovkin
Hemicellulose	130.65 ± 10	129.56 ± 5	127.60 ± 2
Cellulose	176.48 ± 9	173.74 ± 2	175.28 ± 7
Lignin	200.36 ± 12	197.21 ± 5	199.52 ± 1

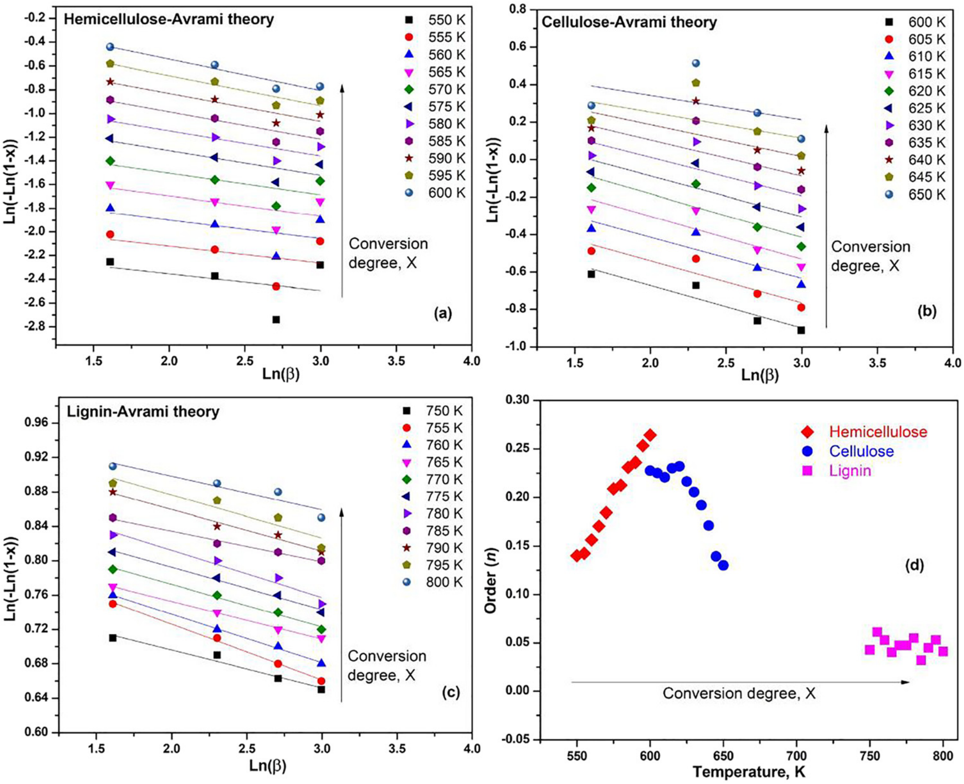

Fig. 8. Regression lines to reaction order (n) proposed by Avrami theory for RW, (a) hemicellulose, (b) cellulose, (c) lignin, and (d) the order variation versus temperature

Table 6. Reaction order and correlation coefficient deduced from Avrami theory for hemicellulose, cellulose and lignin of redwood

Hemicellulose			Cellulose			Lignin		
Temperature	Order (n)	R^2	Temperature	Order (n)	R^2	Temperature	Order (n)	R^2
550	0.140	0.890	600	0.227	0.951	750	0.042	0.950
555	0.142	0.916	605	0.225	0.960	755	0.061	0.994
560	0.156	0.958	610	0.220	0.955	760	0.053	0.996
565	0.170	0.981	615	0.230	0.900	765	0.040	0.997
570	0.184	0.957	620	0.232	0.794	770	0.047	0.985
575	0.208	0.960	625	0.216	0.892	775	0.047	0.941
580	0.212	0.949	630	0.205	0.918	780	0.054	0.980
585	0.231	0.908	635	0.205	0.941	785	0.031	0.970
590	0.236	0.857	640	0.192	0.946	790	0.044	0.840
595	0.253	0.904	645	0.176	0.812	795	0.053	0.839
600	0.264	0.900	650	0.170	0.801	800	0.041	0.810

Table 7. Pre-exponential factor (A) for hemicellulose, cellulose and lignin of redwood

Hemicellulose		Cellulose		Lignin	
Conversion degree (x)	Expo-factor (A) $\times 10^{12}$ s^{-1}	Conversion degree (x)	Expo-factor (A) $\times 10^{14}$ s^{-1}	Conversion degree (x)	Expo-factor (A) $\times 10^{16}$ s^{-1}
0.10	0	0.10	0.10	0.10	3.070
0.15	0	0.15	0.12	0.15	3.076
0.20	0.089	0.20	0.14	0.20	3.115
0.25	0.357	0.25	0.18	0.25	3.173
0.30	0.535	0.30	0.20	0.30	3.269
0.35	0.892	0.35	0.22	0.35	3.270
0.40	1.160	0.40	0.184	0.40	3.307
0.45	1.517	0.45	0.20	0.45	3.450
0.50	1.607	0.50	0.162	0.50	3.461
0.55	2.5	0.55	0.142	0.55	3.470
0.60	1.428	0.60	0.12	0.60	3.500
0.65	2.5	0.65	0.17	0.65	3.557
0.70	1.696	0.70	0.28	0.70	3.692

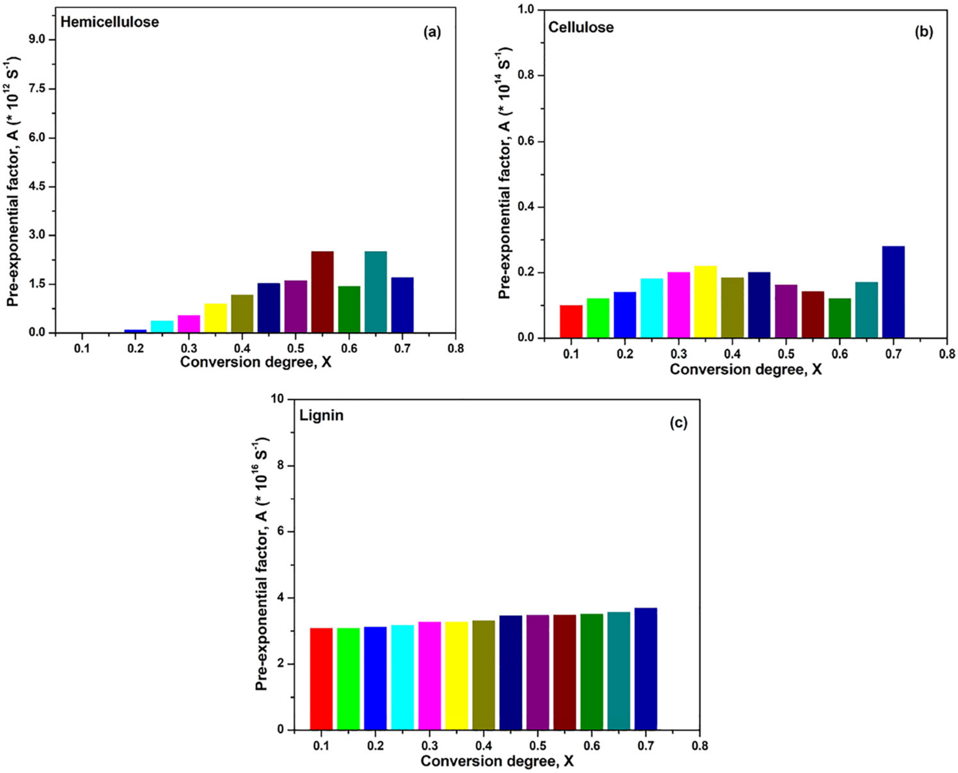

Fig. 9. Variation of pre-exponential factor versus degree of conversion for components of RW, (a) hemicellulose, (b) cellulose and (c) lignin

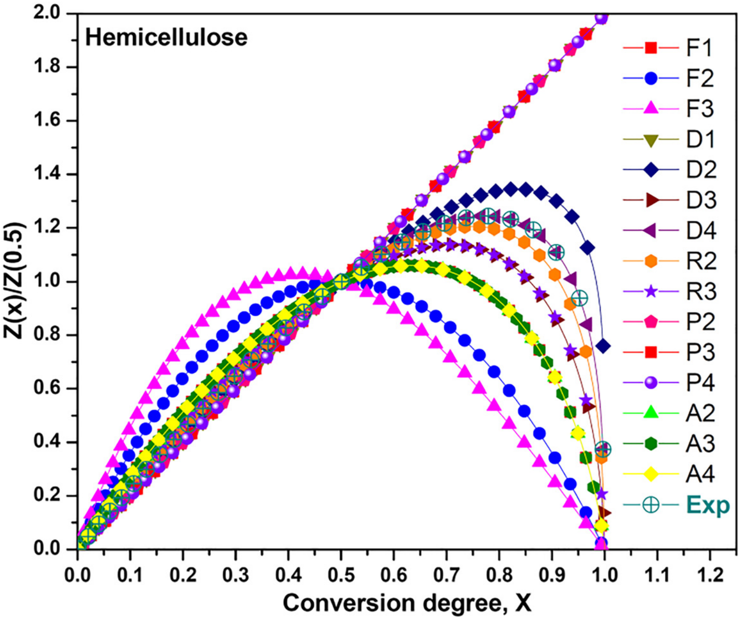

Fig. 10. Master curves for theoretical Z(x)/Z(0.5) and experimental master curve for the degradation of hemicellulose at 10 K min^{-1}

by the increasing of reaction order to a maximum (temperature of 620 K) and then decreases with the increasing the temperature of pyrolysis (up 650 K). The reaction order for cellulose was increased from 0.22 to 0.23, and then decreased to 0.17 with the increase of pyrolysis temperature from 600 to 650 K. Finally, the lignin component was characterized by an arbitrary variation (Fig. 8d). All lignin reaction order values varied from 0.03 to 0.06 with the increase of temperature from 750 to 800 K. The mean values of reaction order (n) calculated were 0.20 for hemicellulose, 0.209 for cellulose and 0.047 for lignin components. Anca-Couce et al. (2020) have worked on biomass pyrolysis TGA assessment with an international round Robin (Anca-Couce et al., 2020). They have showed that reaction order (n) varies with the variation of heating rates (from 1 K min^{-1} to 20 K min^{-1}), and depending on the type of biomass and the pseudo-components. They have concluded that the difference in compositions between hemicellulose, cellulose and lignin influences the kinetic parameters and the thermal decomposition.

According to the Kissinger method (Kissinger, 1957), the eq. (15) was used which the aim to determine the pre-exponential factor *(A)*. Table 7 and Fig. 9 show the results obtained of pre-exponential factor at different conversion degree ($0.1 \le x \le 0.7$) for pseudo-components of redwood biomass. The mean values obtained for pre-exponential factor obtained were 1.09×10^{12} s^{-1}, 0.17×10^{14} s^{-1} and 3.33×10^{16} s^{-1} for hemicellulose, cellulose and lignin, respectively. This variation of pre-exponential (A) for the three components can be explained by the aggregate and structure composition of the RW biomass and the difficult thermal decomposition behavior of the cellulose, hemicellulose and lignin. Tabal et al. (2021) have worked on pyrolysis of Ficus nitada wood biomass; they have determined kinetic parameters from thermogravimetric

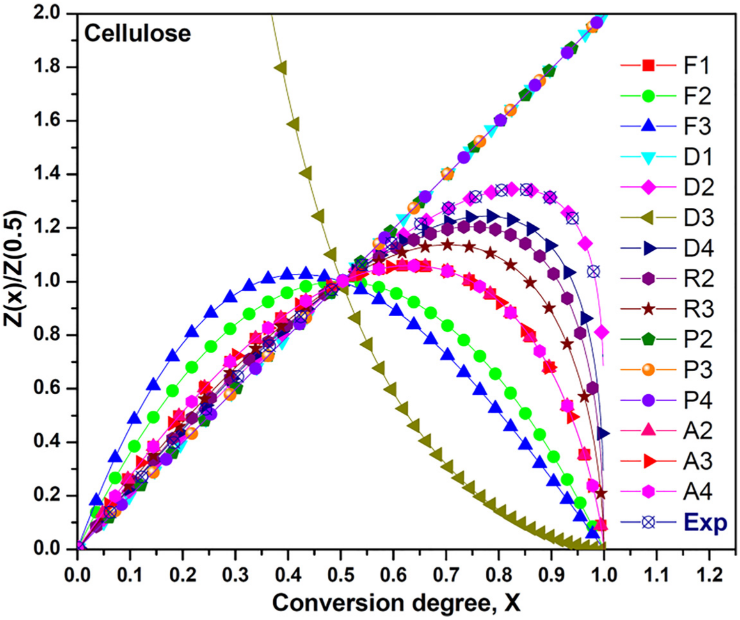

Fig. 11. Master curves for theoretical Z(x)/Z(0.5) and experimental master curve for the degradation of cellulose at 10 K min^{-1}

data of ficus wood biomass (Tabal et al., 2021). The mean values of pre-exponential factors have been $1.12 \times 10^{12}\ \text{s}^{-1}$, $1.14 \times 10^{14}\ \text{s}^{-1}$ and $3.40 \times 10^{14}\ \text{s}^{-1}$ for hemicellulose, cellulose and lignin, respectively. Several researches have mentioned that the pre-exponential factor is proportional to the energy of activation, and there are kinetic compensation effects between the pre-exponential factor and the activation's energy, that can be interpreted by a linear relationship (Tabal et al., 2021; Anca-Couce et al., 2016; 2020).

Reaction mechanism of RW biomass' components

The integral master-plots have been used to reveal and to estimate the kinetic models *f(x)* for hemicellulose, cellulose and lignin's RW biomass components. Figures 10–12 show the plot of experimental and theoretical master plots. According to eq. (19), the associated expressions *g(x)* and *f(x)* that are listed in Table 2 were used to plot master plots *Z(x)*/*Z*(0.5) versus degree of conversion *(x)* for different mechanism. As can be seen, the comparison of experimental master plots obtained at 10 K min^{-1} with the theoretical master plots, thermochemical degradation models of hemicellulose, cellulose and lignin can be revealed and estimated. As can be seen in Figs 10–12, the comparison between theoretical curves and experimental master curve for the decomposition of RW's three components indicates that hemicellulose can be described by the D_4 kinetic model, the cellulose compound can be described by D_2 and the lignin component can be associated to F_3 kinetic model. Kumar Singh et al. (2021) and Tabal et al. (2021), have worked on rice bowl and ficus nitida wood biomass, respectively. They have used master plots to determine the kinetic models of hemicellulose, cellulose and lignin components; they have

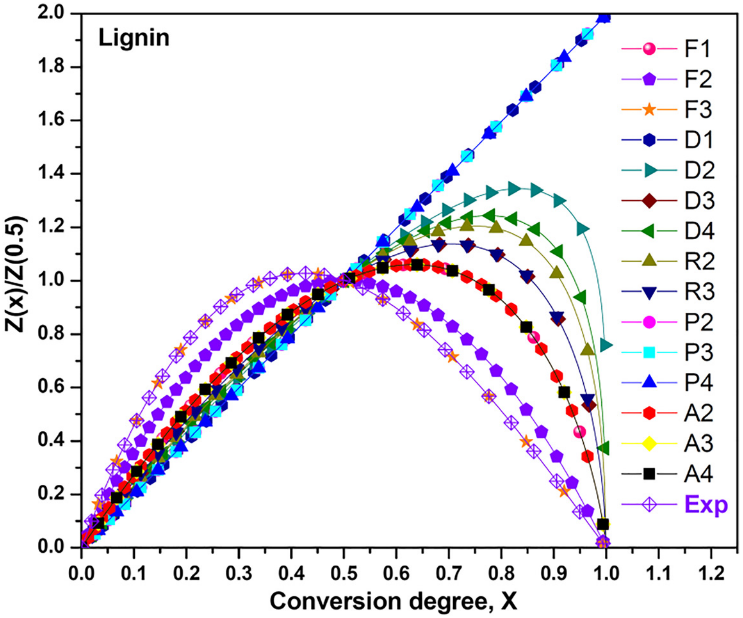

Fig. 12. Master curves for theoretical Z(x)/Z(0.5) and experimental master curve for the degradation of lignin at 10 K min^{-1}

concluded that kinetic model *f(x)* that describes the thermochemical decomposition of biomass, depends on the nature of the biomass through thermogravimetric analaysis process and the percentage of cellulose, hemicellulose and lignin components, and ash percentage (Kumar Singh et al., 2021; Tabal et al., 2021).

CONCLUSION

In this study, the thermal decomposition of RW biomass (*P. sylvestris* L.) was analyzed using the thermogravimetric analysis study. The aim was to provide information about the possibility to convert this type of RW to chemical raw products and to bio-fuel products. The thermal analysis, kinetic modeling and thermochemical parameters were investigated using the thermogravimetric analyzer under nitrogen flow at different heating rates of 5 K min^{-1}, 10 K min^{-1}, 15 K min^{-1} and 20 K min^{-1}.

The pyrolysis of RW biomass has been characterized by three stages of decomposition, which are hemicellulose, cellulose and lignin degradations. In an interval of conversion degree ranging from 10% to 70% ($0.1 \leq x \leq 0.7$), kinetic analysis of this type of wood has indicated that the average energy of activations for the thermochemical decomposition of hemicellulose, cellulose and lignin components were 127.60–130.65 KJ mol^{-1}, 173.74–176.48 KJ mol^{-1} and 197.21–200.36 KJ mol^{-1}, respectively. Through varied temperatures from 550 to 600 K for hemicellulose, from 600 to 650 K for cellulose and from 750 to 800 K for lignin, the mean values of reaction order (n) were 0.20, 0.209 and 0.047 for hemicellulose, cellulose and lignin, respectively. The typical average of pre-exponential factor values (A) for three pseudo-components of redwood biomass were ranged from $0.08 \times 10^{12}\ s^{-1}$ to $2.5 \times 10^{12}\ s^{-1}$, from $0.10 \times 10^{14}\ s^{-1}$ to $0.28 \times 10^{14}\ s^{-1}$ and from $3.07 \times 10^{16}\ s^{-1}$ to $3.69 \times 10^{16}\ s^{-1}$ for hemicellulose, cellulose and lignin, respectively. The probable kinetic models for the thermal decomposition of all three pseudo-components of RW biomass were F_3, D_2 and D_4 for lignin, cellulose and hemicellulose, respectively.

From these kinetic parameters, it can be concluded that *P. sylvestris* RW biomass has interesting properties and can be used as a renewable source of energy and as feedstock in biofuels production.

Credit authorship contribution statement: N. Anter: Investigation. M. Y. Guida: Conceptualization, Format analysis, Writing original draft, Writing-review & Supervision. M. Kasbaji: Investigation. A. Chennani: Investigation. A. Medaghri-Alaoui: Conceptualization, Writing-review & editing. E. M. Rakib: Conceptualization, Writing-review & editing. A. Hannioui: Conceptualization, Supervision, Investigation, Writing-review, Project administration & editing.

Declaration of competing interest: The authors declare that they have no known competing financial interests or personal relationships that could have appeared to influence the work reported in this paper.

ACKNOWLEDGMENTS

All thanks are addressed to the director of organic and analytical chemistry laboratory (LCOA), Pr. A. HANNIOUI, for his invaluable support in this work from a financial and material point of view. And great thanks have been addressed to: Pr. Mr. E. M. Rakib, and Pr. Mr. A. Medaghri-Alaoui, professors of education, members of Educational Committee of Chemistry and Environment Department, Faculty of Sciences and Techniques (FST-BM) and Higher School of Technology (EST-FBS), University of Sultan Moulay Slimane (USMS), for their encouragement and support during the course of this scientific work.

REFERENCES

Akhtar, J. and Saidina Amin, N. (2012). A review on operating parameters for optimum liquid oil yield in biomass pyrolysis. *Renewable & Sustainable Energy Reviews*, 16: 5101–5109.

Anca-Couce, A. (2016). Reaction mechanisms and multi-scale modelling of lignocellulosic biomass pyrolysis. *Progress in Energy and Combustion Science*, 53: 41–79.

Anca-Couce, A., Tsekos, C., Retschitzegger, S., Zimbardi, F., Funke, A., Banks, S., Kraia, T., Marques, P., Scharler, R., De Jong, W., and Kienzl, N. (2020). Biomass pyrolysis TGA assessment with an international round robin. *Fuel*, 276: 118002.

Anca-Couce, A., Berger, A., and Zobel, N. (2014). How to determine consistent biomass pyrolysis kinetics in a parallel reaction scheme. *Fuel*, 123: 230–240, https://doi.org/10.1016/j.fuel.2014.01.014.

Antal, M.J., Varhegyi, G., and Jakab, E. (1998). Cellulose pyrolysis kinetics: revisited. *Industrial & Engineering Chemistry Research*, 37(4): 1267–1275.

Asadullah, M., Rahman, M.A., Ali, M.M., Rahman, M.S., Morin, M.A., Sultan, M.B., and Alam, M.R. (2007). Production of bio-oil from fixed bed pyrolysis of bagasse. *Fuel*, 86: 2514–2520.

Bayramzadeh, S. and Aghaei, P. (2020). Technology integration in complex healthcare environments: a systematic literature review. *Applied Ergonomics*, 92: 103351.

Benedek, J., Sebestyen, T.T., and Bartok, B. (2018). Evaluation of renewable energy sources in peripheral areas and renewable energy based rural development. *Renewable & Sustainable Energy Reviews*, 90: 516–535.

Branca, C., Albano, A., and Di Blasi, C. (2005). Critical evaluation of global mechanisms of wood devolatilization. *Thermochim Acta*, 429(2): 133–141.

Cai, J., Wu, W., Liu, R., and Huber, G.W. (2013). A distributed activation energy model for the pyrolysis of lignocellulosic biomass. *Green Chemistry*, 15(5): 1331. https://doi.org/10.1039/c3gc36958g.

Chen, Y.-C., Chen, W.-H., Lin, B.-J., Chang, J.-S., and Ong, H.C. (2016). Impact of torrefaction on the composition, structure and reactivity of a microalga residue. *Appl Energy*, 181: 110e9.

Chen, Z., Hu, M., Zhu, X., Guo, D., Liu, S., Hu, Z., Xiao, B., Wang, J., and Laghari, M. (2015). Characteristics and kinetic study on pyrolysis of five lignocellulosic biomass via thermogravimetric analysis. *Bioresource Technology*, 192: 441–450.

Doyle, C.D. (1961). Kinetic analysis of thermogravimetric data. *Journal of Applied Polymer Science*, 5: 285–292, https://doi.org/10.1002/app.1961.070051506.

Doyle, C.D. (1965). Series approximations to the equation of thermogravimetric data. *Nature*, 207(4994): 290–291.

Duan, D., Zhang, Y., Wang, Y., Lei, H., Wang, Q., and Ruan, R. (2020). Production of renewable jet fuel and gasoline range hydrocarbons from catalytic pyrolysis of soapstock over corn cob-derived activated carbons. *Energy*, 209: 118454.

Friedman, H.L. (1964). Kinetics of thermal degradation of char-forming plastics from thermogravimetry. Application to a phenolic plastic. *Journal of Polymer Science Part C: Polymer Symposia; Wiley Online Library*.

Gronli, M., Antal, M.J., and Varhegyi, G. (1999). A round-robin study of cellulose pyrolysis kinetics by thermogravimetry. *Industrial & Engineering Chemistry Research*, 38(6): 2238–2244.

Grønli, M.G., Varhegyi, G., and Di Blasi, C. (2002). Thermogravimetric analysis and devolatilization kinetics of wood. *Industrial & Engineering Chemistry Research*, 41(17): 4201–4208.

Guida, M.Y., Bouaik, H., Tabal, A., Hannioui, A., Solhy, A., Barakat, A., Aboulkas, A., and El harfi, K. (2015). Thermochemical treatment of olive mill solid waste and olive mill wastewater: kinetic study. *Journal of Thermal Analysis and Calorimetry*, 123: 1657–1666.

Guida, M.Y., Bouaik, H., EL Mouden, L., Moubarik, A., Aboulkas, A., El Harfi, K., and Hannioui, A. (2017). Utilization of starink approach and avrami theory to evaluate the kinetic parameters of the pyrolysis of olive mill solid waste and olive mill wastewater. *Journal of Advanced Chemical Engineering*, 7: 1–8.

Guida, M.Y., Lanaya, S.E., Rbihi, Z., and Hannioui, A. (2019). Thermal degradation behaviors of sawdust wood waste: pyrolysis kinetic and mechanism. *Journal of Materials and Environmental Science*, 10(8): 742–755.

Guida, M.Y., Lanaya, S.E., Laghchioua, F.E., Rbihi, Z., and Hannioui, A. (2020). Production of bio-oil and bio-char from pyrolysis of sawdust wood waste (SWW). *Progress in Agricultural Engineering Sciences*, 16(1): 61–80.

Guida, M.Y., Rebbah, B., Anter, N., Medaghri-alaoui, A., Rakib, E.M., and Hannioui, A. (2021). Biofuels and biochars production from agricultural biomass wastes by thermochemical conversion technologies:

thermogravimetric analysis and pyrolysis studies. *Progress in Agricultural Engineering Sciences*, 17(1): 15–36.

Hu, M., Chen, Z., Wang, S., Guo, D., Ma, C., Zhou, Y., Chen, J., Laghari, M., Fazal, S., Xiao, B., Zhang, B., and Ma, S. (2016). Thermogravimetric kinetics of lignocellulosic biomass slow pyrolysis using distributed activation energy model, Fraser–Suzuki deconvolution, and iso-conversional method. *Energy Convers Manage*, 118: 1–11. https://doi.org/10.1016/j.enconman.2016.03.058.

Huang, Y.F., Chiueh, P.T., and Lo, S.L. (2016). A review on microwave pyrolysis of lignocellulosic biomass. *Sustainable Environment Research*, 26(3): 103–109.

Ioannidou, O., Zabaniotou, A., Antonakou, E.V., Papazisi, K.M., Lappas, A.A., and Athanassiou, C. (2009). Investigating the potential for energy, fuel, materials and chemicals production from corn residues (cobs and stalks) by non-catalytic and catalytic pyrolysis in two reactor configurations. *Renewable and Sustainable Energy Reviews*, 13: 750–762.

Kaur, R., Gera, P., Jha, M.K., and Bhaskar, T. (2018). Pyrolysis kinetics and thermodynamic parameters of castor (Ricinuscommunis) residue using thermogravimetric analysis. *Bioresource Technology*, 250: 422–428.

Khan, H., Khan, I., and Tienbinh, T. (2020). The heterogeneity of renewable energy consumption, carbon emission and financial development in the globe: a panel quantile regression approach. *Energy Reports*, 6: 859–867.

Kissinger, H.E. (1957). Reaction kinetics in differential thermal analysis. *Analytical Chemistry*, 29: 1702–1706.

Klaas, M., Greenhalf, C., Ouadi, M., Jahangiri, H., Hornung, A., Briens, C., and Berruti, F. (2020). The effect of torrefaction pre-treatment on the pyrolysis of corn cobs. *Results in Engineering*, 7: 100165.

Kumar Singh, R., Patil, T., Verma, A., Tekade, S.P., and Swarkar, A.N. (2021). Insights into kinetics, reaction mechanism, and thermodynamic analysis of pyrolysis of rice straw from rice bowl of India. *Biressource Technology Reports*, 13: 100639.

Kumar Varma, A., Thakur, L.S., Shankar, R., and Mondal, P. (2019). Pyrolysis of wood sawdust: effects of process parameters on products yield and characterization of products. *Waste Management*, 89: 224–235.

Liew, J.X., Minh Loy, A.C., Fui Chin, B.L., Ainouss, A., Shahbaz, M., Al-Ansari, T., Govindan, R., and Chai, Y.H. (2021). Synergistic effects of catalytic co-pyrolysis of corn cob and HDPE waste mixtures using weight average global process model. *Renewable Energy*, 170: 948–963.

Liu, J.G., Jiang, X.M., Zhou, L.S., Han, X.X., and Cui, Z.G. (2009). Pyrolysis treatment of oil sludge and model-free kinetics analysis. *Journal of Hazardous Materials*, 161: 1208–1215.

Mafu Lihle, D., Hein, W.J.P., Neomagus, Raymond, C., Everson, G.N., Okolo, Christien, A., Strydom, and Bunt John, R. (2018). The carbon dioxide gasification characteristics of biomass char samples and their effect on coal gasification reactivity during co-gasification. *Bioresource Technology*, 258: 70e8.

Malakar, A., Kanel, S.R., Ray, C., Snow Daniel, D., and Nadagouda, M.N. (2021). Nanomaterials in the environment, human exposure pathway, and health effects: a review. *Science of Total Environment*, 759: 143470.

Meshitsuka, G. and Isogai, A. (1996). Chemical structures of cellulose, hemicellulose and lignin. In: Hon, D.N. (Ed.), *Chemical modification of lignocellulosic materials*. Marcel Dekker Inc., New York, pp. 11–34.

Minkova, V., Razvigorova, M., Bjornbom, E., Zanzi, R., Budinova, T., and Petrov, N. (2001). Effect of water vapour and biomass nature on the yield and quality of pyrolysis products from biomass. *Fuel Processing Technology*, 70: 53–61.

Mishra, G., Kumar, J., and Bhaskar, T. (2015). Kinetic studies on the pyrolysis of pinewood. *Bioresource Technology*, 182: 282–288.

Moham, D., Pittman, C.U., and Steel, P.H. (2006). Pyrolysis of wood/biomass for bio-oil: a critical review. *Energy & Fuels*, 20: 848–889.

Moya, R., Rodríguez-Zúñiga, A., Puente-Urbina, A., and Gaitán-Álvarez, J. (2018). Study of light, middle and severe torrefaction and effects of extractives and chemical compositions on torrefaction process by thermogravimetric analysis in five fast-growing plantations of Costa Rica. *Energy*, 149: 1e10.

Mu, L., Chen, J., Yin, H., Song, X., Li, A., and Chi, X. (2015). Pyrolysis behaviors and kinetics of refining and chemicals wastewater, lignite and their blends through TGA. *Bioresource Technology*, 180: 22–31.

Mullen, C.A., Boateng, A.A., Goldberg, N.M., Lima, I.M., Laird, D.A., and Hicks, K.B. (2010). Bio-oil and bio char production from corn cobs and stover by fast pyrolysis. *Biomass and Bioenergy*, 34: 67–74.

Ozawa, T. (1965). A new method of analyzing thermogravimetric data. *Bulletin of the Chemical Society of Japan*, 38(11): 1881–1886.

Ozbay, N., Putun, A.E., Uzun, B.B., and Putun, E. (2001). Biocrude from biomass: pyrolysis of cottonseed cake. *Renewable Energy*, 24(3–4): 615–625.

Phuakpunk, K., Chalermsinsuwan, B., and Assabumrungrat, S. (2020). Comparison of chemical reaction kinetic models for corn cob pyrolysis. *Energy Reports*, 6: 168–178.

Pimenta, A.S., Da Costa Monteiro, T.V., Fasciohi, M., Braga, R.M., De Souza, E.E., and De lina, K.M.G. (2018). Fast pyrolysis of trunk wood and stump wood from a Brazilian eucalyptus clore. *Industrial Crops and Products*, 125: 630–638.

Poletto, M. (2016). Thermogravimetric analysis and kinetic study of pine wood pyrolysis. *Ciência da Madeira (Brazilian Journal of Wood Science)*, 7(2): 111–118.

Rout, T., Pradhan, D., Singh, R.K., and Kumari, N. (2016). Exhaustive study of products obtained from coconut shell pyrolysis. *Journal of Environmental Chemical Engineering*, 4: 3696–3705.

Sanchez-Jimenez, P.E., del Rocio Rodriguez-Laguna, M., Perez-Maqueda, L.A., and Criado, J.M. (2014). Comments on “Pyrolysis kinetics of biomass from product information”(Applied Energy 110 (2013) 1–8) regarding the inability to obtain meaningful kinetic parameters from a single non-isothermal curve. *Applied Energy*, 125: 132–135.

Sensoz, S., Demiral, I., and Gercel, H.F. (2006). Olive bagasse (oleaeuropa L.) pyrolysis. *Bioresource Technology*, 97: 429–436.

Shang, H., Du, W., Liu, Z., and Zhang, H. (2013). Development of microwave induced hydrodesulfurization of petroleum streams: a review. *Journal of Industrial and Engineering Chemistry*, 19(4): 1061–1068.

Situmorang, Y.A., Zhao, Z., Chaihad, N., Wang, C., Anniwaer, A., Kassai, Y., Abudula, A., and Guand, G. (2021). Steam gasification of co-pyrolysis chars from various types of biomass. *The International Journal of Hydrogen Energy*, XX: 1–11.

Slopiecka, K., Bartocci, P., and Fantozzi, F. (2012). Thermogravimetric analysis and kinetic study of poplar wood pyrolysis. *Applied Energy*, 97: 491–497.

Tabal, A., Barakat, A., Aboulkas, A., and Elharfi, K. (2021). Pyrolysis of ficus nitida wood: determination of kinetic and thermodynamic parameters. *Fuel*, 283: 113253.

Uzun, B.B., Putun, A.E., and Putun, E. (2007). Composition of products obtained via fast pyrolysis of olive oil residue: effect of pyrolysis temperature. *Journal of Analytical and Applied Pyrolysis*, 79: 147–153.

Vyazovkin, S. (2006). Model-free kinetics. *Journal of Thermal Analysis and Calorimetry*, 83(1): 45–51.

Vyazovkin, S. and Lesnikovick, A. (1988). Transformation of “degree of conversion against temperature” into “degree of conversion against time” kinetic data. *Russian Journal of Physical Chemistry A*, 62(1525): e7.

Watt, E., Abdelwahab, M.A., Mohanty, A.K., and Misra, M. (2020). Biocomposites from biobased polyamide 4, 10 and waste corn cob based bio-carbon. *Composites, JCOMA*.

White, J.E., Catallo, W.J., and Legendre, B.L. (2011). Biomass pyrolysis kinetics: a comparative critical review with relevant agricultural residue case studies. *Journal of Analytical and Applied Pyrolysis*, 91(1): 1–33.

Worasuwannarak, N., Sonobe, T., and Tanthapanichakoon, W. (2007). Pyrolysis behaviors of rice straw, rice husk, and corncob by TG-MS technique. *Journal of Analytical and Applied Pyrolysis*, 78: 265–271.

Xiao, Y., Pudasainee, D., Gupta, R., Xu, Z., and Diao, Y. (2017). Bromination of petroleum coke for elemental mercury capture. *Journal of Hazardous Materials*, 33b: 232–239.

Xin, X., Dell, K., Udugama, I.A., Young, B.R., and Baroutiau, S. (2020). Transforming biomass pyrolysis technologies to produce liquid smoke food flavouring. *Journal of Cleaner Production*, XX: 1–12.

Yanting, Z., and Liyun, X. (2011). Research on risk management of petroleum operations. *Energy Procedia*, 5: 2330–2334.

Zabaniotou, A.A. (2010). Pyrolysis of forestry biomass by-products in Greece. *Energy Sources*, 21: 395–403.

Zhou, H., Long, Y.Q., Meng, A.H., Li, Q.H., and Zhang, Y.G. (2013). The pyrolysis simulation of five biomass species by hemi-cellulose, cellulose and lignin based on thermogravimetric curves. *Thermochim Acta*, 566: 36e43.
